Cerebral Cortex February 2011;21:401–412
doi:10.1093/cercor/bhq115
Advance Access publication June 24, 2010

L1 and CHL1 Cooperate in Thalamocortical Axon Targeting

Galina P. Demyanenko[1,2], Priscila F. Siesser[1,2], Amanda G. Wright[1,2,3], Leann H. Brennaman[1,2], Udo Bartsch[4], Melitta Schachner[5] and Patricia F. Maness[1,2]

[1]Department of Biochemistry and Biophysics, [2]Neuroscience Research Center, University of North Carolina School of Medicine, Chapel Hill, NC 27599, USA, [3]Department of Biology, Marymount University, Arlington, VA 22207, USA, [4]Department of Ophthalmology, University Medical Centre Hamburg-Eppendorf, 20246 Hamburg, Germany and [5]Department of Cell Biology and Neuroscience, Rutgers University, Piscataway, NJ 08854, USA

Demyanenko, Siesser, and Wright have contributed equally to this work

Address correspondence to Patricia F. Maness. Email: srclab@med.unc.edu.

Neural cell adhesion molecule close homolog of L1 (CHL1) is a regulator of topographic targeting of thalamic axons to the somatosensory cortex (S1) but little is known about its cooperation with other L1 class molecules. To investigate this, CHL1$^{-/-}$/L1$^{-/y}$ double mutant mice were generated and analyzed for thalamocortical axon topography. Double mutants exhibited a striking posterior shift of axons from motor thalamic nuclei to the visual cortex (V1), which was not observed in single mutants. In wild-type (WT) embryos, L1 and CHL1 were coexpressed in the dorsal thalamus (DT) and on fibers along the thalamocortical projection in the ventral telencephalon and cortex. L1 and CHL1 colocalized on growth cones and neurites of cortical and thalamic neurons in culture. Growth cone collapse assays with WT and mutant neurons demonstrated a requirement for L1 and CHL1 in repellent responses to EphrinA5, a guidance factor for thalamic axons. L1 coimmunoprecipitated with the principal EphrinA5 receptors expressed in the DT (EphA3, EphA4, and EphA7), whereas CHL1 associated selectively with EphA7. These results implicate a novel mechanism in which L1 and CHL1 interact with individual EphA receptors and cooperate to guide subpopulations of thalamic axons to distinct neocortical areas essential for thalamocortical connectivity.

Keywords: axon guidance, cell adhesion molecule, Ephrin, L1, thalamocortical axon mapping

Introduction

L1 family neural cell adhesion molecules (L1-CAMs) are immunoglobulin (Ig) class transmembrane receptors with critical functions in neurodevelopment. Members of this family—L1, close homolog of L1 (CHL1), NrCAM, and neurofascin—are widely expressed in the developing nervous system and regulate axon guidance and synaptic plasticity (Maness and Schachner 2007). L1 mutations at human chromosomal locus Xq28 result in a pleiotropic syndrome of mental retardation (Kenwrick et al. 2000), and the human homolog of CHL1 at 3p26.1 (CALL) is implicated in the 3p-syndrome of low IQ and developmental delay (Frints et al. 2003). L1 null mutant mice display errors of axon guidance in the corticospinal tract (CST) (Dahme et al. 1997; Cohen et al. 1998), corpus callosum (Demyanenko et al. 1999), and retinocollicular projection (Demyanenko and Maness 2003; Buhusi et al. 2008), and they are learning impaired (Fransen et al. 1998). CHL1 null mutant mice show aberrant thalamocortical projections (Wright et al. 2007), abnormal positioning of cortical neurons (Demyanenko et al. 2004), deficits in cognitive processing of spatial information (Montag-Sallaz et al. 2002), attention, sensory gating (Pratte et al. 2003; Irintchev et al. 2004), and working memory (Kolata et al. 2008). L1 and CHL1 phenotypes differ, but they have not been examined for an ability to cooperate in guiding axons to synaptic targets. To this end, we generated L1/CHL1 double mutant mice and analyzed the combined effect of loss of both L1-CAMs on topographic mapping of thalamocortical axons.

The topographic projection of axons from discrete nuclei in the dorsal thalamus (DT) to specific neocortical areas is vital for proper cortical connectivity. Topographic mapping of the thalamocortical projection is organized along 2 axes. During embryogenesis, thalamic afferents originating in rostral thalamic nuclei, the ventroanterior (VA) and ventrolateral (VL) nuclei, project to rostromedial neocortical areas; while axons from caudal thalamic nuclei, such as the dorsal lateral geniculate nucleus (LGN) project to caudolateral areas (Price et al. 2006). CHL1 has been shown to regulate topographic mapping of thalamic axon contingents from the ventrobasal (VB) complex located in the middle of the DT to the primary somatosensory cortex (S1), specifically mediating thalamic axon guidance at the ventral telencephalon (VTe) (Wright et al. 2007). The VTe is a key intermediate sorting target that directs embryonic thalamic axons toward different rostrocaudal areas of the neocortex (Dufour et al. 2003). Deletion of CHL1 causes a caudal shift within the VTe of axons from the middle DT, resulting in final mistargeting of VB axon contingents to V1 in the caudal region of the neocortex (Wright et al. 2007). CHL1 functions on DT axon subpopulations by mediating repulsive axon guidance to the high-caudal gradient of Semaphorin3A (Sema3A) in the VTe, achieved by serving as a coreceptor for Sema3A by binding Neuropilin-1 (Wright et al. 2007). Because L1 shares significant homology with CHL1 and also mediates Sema3A repulsive responses by binding Neuropilin-1 (Bechara et al. 2008), L1 might coordinate functionally with CHL1 to regulate thalamocortical axon guidance. However, L1-CAMs may have broader roles in repellent guidance by functioning as coreceptors for other axon guidance cues acting in the VTe. In particular, L1-CAMs could conceivably mediate axon repulsion to a high-caudal gradient of EphrinA5 in the VTe, which is known to direct rostral DT axons with elevated expression of EphA receptors to the primary motor cortex (M1) (Dufour et al. 2003). Little is known about interactions of L1-CAMs with EphA receptors in neurons. L1 is involved in reverse signaling through EphrinB in retinal ganglion cells in culture (Suh et al. 2004) and binds EphA4 in platelets (Prevost et al. 2002), but a role in axon guidance in vivo has not been investigated.

To investigate functions for CHL1 and L1 in topographic mapping of thalamocortical axons, we generated a novel

strain of $CHL1^{-/-}/L1^{-/y}$ double mutant mice and analyzed their thalamocortical topographic map by axon tracing. $CHL1^{-/-}/L1^{-/y}$ double mutants exhibited a striking caudal shift of motor DT axons to V1, similar to the phenotype of EphA/EphrinA mutant mice, whereas single mutants did not exhibit this misprojection. Furthermore, L1 and CHL1 were coexpressed on thalamic axons along the developing thalamocortical trajectory, associated with EphA receptors, and mediated EphrinA5-induced growth cone collapse. These results suggest a novel cooperative function for L1 and CHL1 in topographic mapping of thalamic axon populations to the motor cortex by interacting with the EphrinA/EphA repellent guidance system.

Materials and Methods

Mice

The L1 gene is located on the X chromosome, and its deletion results in poor breeding capability of males and thus female mice homozygous null for the CHL1 gene and heterozygous for L1 ($CHL1^{-/-}/L1^{+/-}$; C57BL/6/Sv129, ~9:1) were crossed with $CHL1^{-/-}/L1^{+/y}$ males (C57BL/6) to produce $CHL1^{-/-}/L1^{-/y}$ double mutants. To visualize the boundary between the primary and secondary (V2) visual cortical areas, $CHL1^{-/-}/L1^{+/y}$ mice were intercrossed with Thy1-yellow fluorescent protein (YFP) line H reporter mice (C57BL/6 [Feng et al. 2000]), in which layer V pyramidal cells are labeled in V2 but not V1 (Demyanenko et al. 2004). Resulting $YFP^{+}/CHL1^{-/-}/L1^{+/y}$ males were then crossed with $CHL1^{-/-}/L1^{+/-}$ females (C57BL/6) to produce $YFP^{+}/CHL1^{-/-}/L1^{-/y}$ mutants. Embryonic day 0.5 (E0.5) was defined as the plug date and postnatal day 0 (P0) as the day of birth. Animal care and treatment were in accordance with guidelines provided by the University of North Carolina Institutional Animal Care and Use Committee.

Immunostaining, Analysis of Cortical and Thalamic Areas, and Preparation of Neuronal Cultures

Immunofluorescence staining was conducted using 10-μm frozen sections of mouse brain using antibodies directed against CHL1 (goat polyclonal anti-CHL1, R&D Systems; 1:200) and L1 (rat polyclonal anti-L1, Abcam; 1:50) as described (Demyanenko et al. 1999), with FITC- or rhodamine-conjugated secondary antibodies. The specificity of these antibodies for CHL1 and L1, respectively, in mouse forebrain from E13 through adulthood has been demonstrated (Demyanenko et al. 1999; Nikonenko et al. 2006; Wright et al. 2007; Guseva et al. 2009). Nissl staining was carried out on 40-μm brain sections as described (Demyanenko et al. 1999).

For preparation of neuronal cultures, cortical or thalamic neurons (E14.5) were dissociated by trituration using a fire-polished Pasteur pipette. Cells were plated on poly-D-lysine, and fibronectin-coated chamber slides in Dulbecco's modified Eagle's medium (DMEM) supplemented with 10% fetal bovine serum. One day after plating, the media was changed to Neurobasal media containing B27 supplement and glutamate (25 μM). After 72 h, cortical cells were fixed in 4% *paraformaldehyde* (PFA) and permeabilized with 0.05% Triton in phosphate-buffered saline (PBS). Thalamic cells were fixed in methanol/acetone (1:1). After blocking in 10% donkey serum/PBS, cells were double stained with antibodies against L1 (rat polyclonal anti-L1, Abcam; 1:100) and CHL1 (1:100) followed by incubation with TRITC-conjugated donkey anti-rat IgG (1:150) and FITC-conjugated donkey anti-goat IgG (1:150). Staining was analyzed using an Olympus FluoView500 laser scanning confocal microscope.

In Situ Hybridization

cDNA including nucleotides 2866–3523 of L1 cDNA (NM_008478) was subcloned into NotI and KpnI sites in psBluescript SK and used as a template to generate L1 probes. The sense probe was generated by linearizing the plasmid with NotI and transcribing with T3 polymerase. The antisense probe was generated by linearizing the plasmid with KpnI and transcribing with T7 polymerase. Brains from wild-type (WT) embryos (E14.5; C57BL/6) were immersion fixed in 4% PFA overnight and cryoprotected in sucrose before sectioning in the horizontal plane. Alternatively, cryostat sections from unfixed brains were mounted onto slides and fixed with 4% PFA before being subjected to in situ hybridization analysis. In situ hybridization was performed as described using digoxigenin-labeled probes as described (Bartsch et al. 1994).

Retrograde Tracing of Thalamocortical Axons

Retrograde axon tracings were performed as described (Wright et al. 2007) by focal injection of solutions of DiI (1,1′, di-octadecyl-3,3,3′,3′-tetramethylindocarbocyanine perchlorate) or DiA (4,4-dihexadecyl aminostyryl N-methyl-pyridinium iodide) (Invitrogen, Inc.; 5% in ethanol) into the primary motor (M1), somatosensory (S1), or visual (V1) cortical areas of living mice at postnatal day 5 (P5), anesthetized by hypothermia. Injections were made with capillary micropipettes connected to a Picospritzer II. Mice were euthanized 2 days later, and brains were fixed by transcardial perfusion. Forebrains were vibratome sectioned in the coronal plane (100 μm), and injection sites were monitored microscopically. Only injections restricted to the neocortex without entering the white matter were analyzed. Sections were analyzed for labeling of cell bodies of individual thalamic nuclei by epifluorescence and confocal microscopy. 4′,6-diamidino-2-phenylindole nuclear staining was used to identify the position of the thalamic nuclei by comparison with atlas coordinates (Paxinos et al. 2007). Further details of the protocol and analysis are provided in Wright et al. (2007).

Growth Cone Collapse Assay

Growth cone collapse assays were performed as previously described (Wright et al. 2007). Cortical tissue was obtained from WT and $L1^{-/y}$ embryonic brains (E14.5) by microdissection in ice-cold Hank's balanced salt solution (HBSS). Dissociated cortical neurons were produced as described above and subjected to double staining for L1 and CHL1. After culturing for 72 h, cells were treated with either EphrinA5 fused to Fc (EphrinA5-Fc) or nonimmune Ig (control) (30 nM each) for 30 min. Cells were fixed with 4% PFA and actin labeled with rhodamine-conjugated phalloidin (Invitrogen; 1:40). Axons were scored for growth cone collapse by morphological criteria using fluorescence microscopy. Growth cones were scored as collapsed if they had a bullet-shaped morphology, whereas they were scored as uncollapsed if they were well spread and displayed numerous filopodia and lamellipodia. Values represent means ± standard error of the mean. Student's *t*-test was utilized to compare different treatment groups as indicated. $P < 0.05$ was considered significant.

For preparation of explants, WT and $CHL1^{-/-}$ embryonic brains (E14.5) were vibratome sectioned (300 μm), and thalamic regions were obtained by microdissection in ice-cold HBSS. Explants were plated on fibronectin-coated MatTek dishes using a plasma clot (20 μL of bovine thrombin with 20 μL of chicken plasma, Sigma) to ensure adherence of the explants. The explants were cultured for 48 h and treated with either Fc protein fused to alkaline phosphatase (AP) (Fc-AP; 30 nM) or EphrinA5 fused to AP (EphrinA5-AP, 30 nM; [Flanagan and Cheng 2000]) for 30 min. Fc-AP and EphrinA5-AP were prepared by transfecting HEK-293T cells using Lipofectamine 2000 (Needham et al. 2001) and purified as described (Flanagan and Cheng 2000). After 2 days, media was collected and the concentration of the Fc proteins was determined (Flanagan and Cheng 2000). Explants were fixed and stained, growth cone morphology was analyzed using confocal microscopy, and data analysis was performed as described above.

Coimmunoprecipitation

HEK293T cells were maintained in DMEM containing 10% bovine calf serum and transiently transfected with pcDNA3 constructs encoding mouse CHL1, human L1, rat EphA7 (from Dr Masaaki Torii) and mouse EphA3, chicken EphA4, and chicken EphB2 (from Dr Elena Pasquale) using Lipofectamine 2000 as described (Needham et al. 2001). Two days after transfection, HEK293T cells were washed with HBSS and lysed in either RIPA buffer (20 mM Tris–HCl [pH 7.4], 150 mM NaCl, 5 mM ethylenediaminetetraacetic acid [EDTA]-Na, 1 mM

ethyleneglycol-bis(2-aminoethylether)-N,N,N',N'-tetra acetic acid [EGTA]-Na, 1% NP40, 1% sodium deoxycholate, 0.1% sodium dodecyl sulfate [SDS], 10 mM NaF, 10 μg/mL leupeptin, 1% aprotinin, and 0.2 mM Na_3VO_4) or Brij-97 buffer (1% Brij-97, 10 mM Tris–HCl [pH 7.4], 150 mM NaCl, 1 mM EDTA, 1 mM EGTA, 500 μg/mL Pefabloc, 10 mM NaF, 10 μg/mL leupeptin, 1% aprotinin, and 0.2 mM Na_3VO_4). Protein concentrations in the lysates were determined using the BCA protein assay. For immunoprecipitation, 0.5-mL lysate (500 μg) was precleared with nonimmune IgG and A/G agarose beads for 30 min at 4 °C. Supernatants were incubated for 1 h with either normal IgG (control) or 1–2 μg each of specific antibodies, and immune complexes collected after 30-min incubation with protein A/G agarose. The immunoprecipitates were washed with lysis buffer and processed for immunoblotting by separation of samples (25 μg) on 7.5% SDS–polyacrylamide gels and transferred to nitrocellulose membranes. Nonspecific binding was blocked by incubating 1 h in Tris-buffered saline containing 0.05% Tween 20 (TBST) and 5% nonfat dry milk. Membranes were incubated overnight in primary antibody, washed with TBST, and then incubated for 1 h with horse radish peroxidase-conjugated secondary antibody. After 3 washes in TBST, the blots were developed by enhanced chemiluminescence (Amersham Biosciences) and exposed to autoradiographic films.

Results

Generation and Characterization of CHL1$^{-/-}$/L1$^{-/y}$ Double Mutant Mice

To investigate cooperative functional roles for CHL1 and L1 in thalamocortical mapping, CHL1$^{-/-}$/L1$^{-/y}$ double mutant mice were generated. Among offspring, double mutant males were produced at a reduced Mendelian frequency of 8.7%, instead of the expected 25%, but were viable and survived to adulthood. Double mutants (8 weeks of age) were smaller than normal (Fig. 1*A*) with body weights 55–60% of CHL1$^{-/-}$ single mutants or WT mice. L1$^{-/y}$ single mutants have body weights that are 60–80% of WT (Dahme et al. 1997), thus the smaller size of the double mutants most likely reflected the loss of L1. Because L1 and CHL1 are also expressed in some hematopoietic cells and elsewhere outside the brain (Maness and Schachner 2007), immune dysfunction or some other deficiency may contribute to the reduced body size of mutant mice. The cerebral cortex of CHL1$^{-/-}$/L1$^{-/y}$ double mutants (postnatal day 21; P21) had a normal thickness and laminar neuronal distribution in all neocortical areas, as shown in the primary somatosensory cortex (S1) (Fig. 1*B*). The double mutant brain also displayed grossly normal neuroanatomy in the cerebral cortex, hippocampus, corpus callosum, cerebellum, ventricles, thalamus, optic nerve, and olfactory bulb (not shown). Nissl staining showed normal positioning of M1 in double mutants (P7) with typical barrels (Fig. 1*C–Dd*, circled), as well as normally positioned thalamic nuclei VL, VB, mediodorsal (Fig. 1*H,I*), and dLGN (Fig. 1*J,K*). To assess potential defects at the V1/V2 boundary that might perturb axon targeting, CHL1$^{-/-}$/L1$^{-/y}$ mice were intercrossed with Thy1-YFP line H reporter mice (Feng et al. 2000), in which layer V pyramidal cells express YFP in V2 but not V1, thus marking the boundary between these subregions (Demyanenko et al. 2004). CHL1$^{-/-}$/L1$^{-/y}$/YFP^{+} mutants (P21) displayed normal positioning of V1 and V2 compared with WT/YFP^{+} mice (Fig. 1*E–G*). L1 and CHL1 are known to colocalize in the neonatal CST at medullary pyramids and at the pyramidal decussation, and loss of L1 in L1-minus mice results in a size reduction of the CST and impaired decussation (Dahme et al. 1997; Cohen et al. 1998; Runker et al. 2003). Adult CHL1$^{-/-}$/L1$^{-/y}$ double mutant mice, but not CHL1$^{-/-}$ single mutants, exhibited a reduced cross-sectional area of the CST at caudal levels of the medulla but the size reduction was not significantly greater than in L1$^{-/y}$ mice (not shown).

Colocalization of L1 and CHL1 in the Thalamocortical Pathway

To determine if L1 and CHL1 were coexpressed in mouse embryos during thalamocortical pathfinding, double immunofluorescence staining was carried out in the DT in mouse embryos at E14.5, when thalamic axons extend from the thalamic eminence (TE) through the VTe "en route" to the cortex (Fig. 1*L–N*). L1 and CHL1 were localized on fibers in the DT and were prominent in axons extending through the TE and VTe (Fig. 1*L–N*). In the VTe at higher magnification, many fibers were seen that expressed both L1 and CHL1, but some expressed only L1 and fewer expressed only CHL1 (Fig. 1*O–T*). In the DT (Fig. 1*U–W*), L1 and CHL1 colocalized along much of the rostrocaudal axis; however, CHL1 was preferentially enriched in medially and L1 somewhat enriched laterally. The L1 and CHL1 antibodies have been shown to be specific for each protein and do not label L1$^{-/y}$ or CHL1$^{-/-}$ brain, respectively (Nikonenko et al. 2006; Guseva et al. 2009). L1 and CHL1 were also expressed in the E14.5 neocortex (Fig. 1*L–M* and *X–Z*). These L1-CAMs colocalized in many but not all fibers of the cortical intermediate zone (IZ) and in the marginal zone, with less expression in the cortical plate and little expression in the ventricular zone (Fig. 1*Z*). These experiments confirm and extend results on L1 expression in the E14–18 mouse cortical IZ (Kudo et al. 2005) and on thalamic axons within the E16 rat cortex and internal capsule (Fukuda et al. 1997) by demonstrating colocalization of L1 with CHL1 on specific fibers within the VTe and neocortex. In situ hybridization in the E14.5 DT revealed L1 transcripts throughout the rostrocaudal extent of the DT (Fig. 1*Aa*). L1 transcripts generally occupied a similar DT location as CHL1 transcripts, as shown previously (Wright et al. 2007), although L1 transcripts were more abundant than CHL1 transcripts in the far rostral DT, while CHL1 transcripts were enriched in the central region of the DT (Wright et al. 2007). The rostral DT contains the developing VA and VL motor nuclei, while the central DT contains the developing VB thalamic nuclei, and caudal DT contains the dorsal LGN.

CHL1 and L1 Cooperate to Regulate Thalamocortical Axon Targeting

To investigate whether L1 cooperates with CHL1 in area-specific thalamocortical axon mapping, retrograde axon tracing of WT, homozygous CHL1$^{-/-}$/L1$^{-/y}$ double knockout, and L1$^{-/y}$ mutant mice was performed in live anesthetized mice at postnatal day 5 (P5), when final thalamocortical topography is established (Agmon et al. 1995). Retrograde axon tracing of thalamic axons in postnatal mice was performed by injecting DiI or DiA into different neocortical areas (primary motor [M1], somatosensory [S1], or visual cortex [V1]) then analyzing labeled neuronal cell bodies in thalamic nuclei after 36 h (Fig. 2). The accuracy of all injections was monitored by epifluorescence microscopy. Projections of afferents from DT nuclei to cortical areas in different mouse genotypes are depicted in summary schemes illustrating primarily the rostrocaudal axis (Fig. 2*A–D*), facilitating comparison with horizontal brain sections showing retrograde labeling of DT

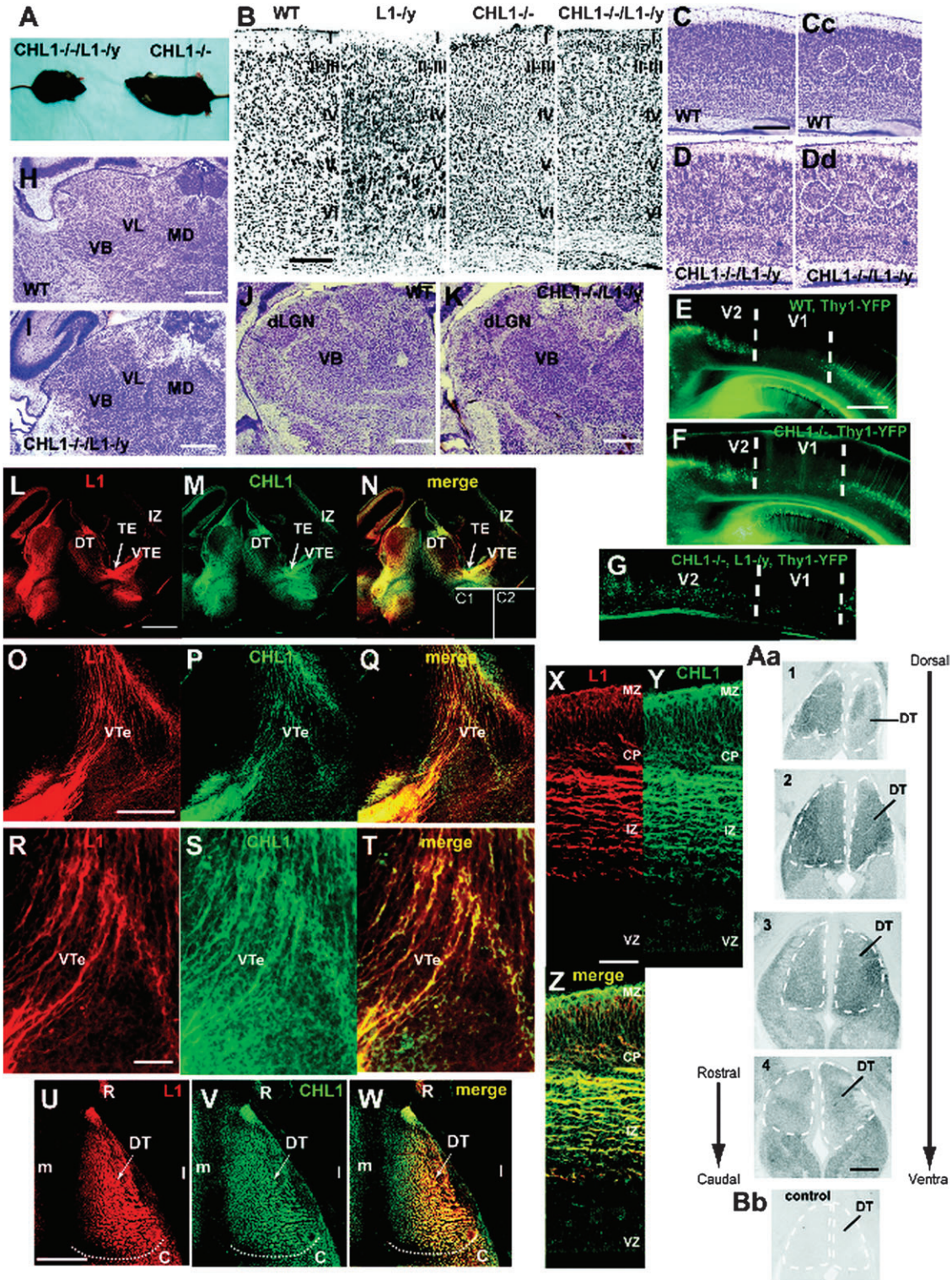

Figure 1. Analysis of CHL1$^{-/-}$/L1$^{-/y}$ double mutant mice and expression of CHL1 and L1 in the thalamocortical pathway. (*A*) CHL1$^{-/-}$/L1$^{-/y}$ double mutant mice are reduced in size compared with CHL1$^{-/-}$ mutant mice. (*B*) Nissl staining of primary somatosensory cortex in WT, L1$^{-/y}$, CHL1$^{-/-}$, and CHL1$^{-/-}$/L1$^{-/y}$ mice (P21) in coronal sections. (*C* and *D*) Nissl staining of S1 cortex in WT (*C*) and CHL1$^{-/-}$/L1$^{-/y}$ mice (*D*) (P7) showing normal barrels (circled in WT *Cc* and mutant *Dd*). (*E–G*) Normal boundary between V1 and V2 visualized by YFP-expressing layer V pyramidal neurons in WT (*E*), CHL1$^{-/-}$ (*F*), and CHL1$^{-/-}$/L1$^{-/y}$ mice crossed to Thy1-YFP (line H) reporter mice at P21. (*H–K*) Normal size and location of DT nuclei visualized by Nissl staining of WT (*H*) and CHL1$^{-/-}$/L1$^{-/y}$ double mutant mice (*I*) at P7. dLGN, dorsal LGN nuclei. (*L–N*) Immunofluorescence staining for L1 and CHL1 in the thalamocortical pathway of WT embryos (E14.5) in midcoronal sections. C1, L1$^{-/y}$ brain stained with L1 antibody. C2, CHL1$^{-/-}$ brain stained with CHL1 antibody. (*O–P*) Immunofluorescence staining for L1 and CHL1 in the VTe of WT embryos (E14.5) in coronal sections. (*R–T*) Higher magnification images of *L–N*. (*U–W*) Immunofluorescence staining for L1 and CHL1 in the DT of WT embryos (E14.5) in horizontal sections. R, rostral; C, caudal; m, medial, l, lateral. (*X–Z*) Immunofluorescence staining for L1 and CHL1 in the neocortex of WT embryos (E14.5). MZ, marginal zone; CP, cortical plate; VZ, ventricular zone. (*Aa*) In situ hybridization for L1 mRNA in serial horizontal sections of WT embryos (E14.5). L1 transcripts were present throughout the DT (dashed lines). (*Bb*) No expression was observed with the sense probe (control). Magnification bar = 100 μm in *B*; 200 μm in *C* and *D*; 500 μm in *Aa*, *E–N*, *U–W*; 300 μm in *O–Q*; 50 μm in *X–Z*.

nuclei. In vivo, rostral DT nuclei such as VA/VL actually project rostromedially to M1, and caudal DT nuclei such as the dorsal LGN, project caudolaterally to V1 (Price et al. 2006). In all WT mice (13 of 13 injections), retrograde labeling of neuronal cell bodies in the DT following single injections of DiI into M1 labeled only VA/VL nuclei and not VB nuclei ventroposterior medial (VPM) and ventroposterior lateral (VPL) (Fig. 2*A1*) or dorsal LGN (not shown) as described before (Molnar et al. 2003; Vanderhaeghen and Polleux 2004; Wright et al. 2007). Dual injection of DiA into S1 and DiI into V1 of WT mice resulted in specific labeling of VB and the dorsal LGN, respectively, also as expected (Fig. 2*A2*).

Retrograde labeling of thalamocortical axons in $L1^{-/y}$ mutants following single DiA injections into M1 labeled only motor thalamic nuclei, VA/VL in 3 out of 3 mice, as shown for VL (Fig. 2*B1*) with no labeling of VB (VPL, VPM) or dorsal LGN. Injections of DiI into S1 of $L1^{-/y}$ mice labeled only VB nuclei in 7 out of 7 injections (Fig. 2*B2*) with no labeling of other DT nuclei. DiI injections into V1 of $L1^{-/y}$ mice showed labeling of only the dorsal LGN with no labeling of motor or somatosensory thalamic nuclei (6 out of 6 injections) (Fig. 2*B3*; inset at higher magnification). Comparison with WT mice above (n = 13 injections) indicated that there were no significant differences (Chi-square, 1 degree of freedom = undefined). Thus, motor, somatosensory, and dorsal LGN thalamic axons projected normally in $L1^{-/y}$ mice. These results were in accord with a thalamocortical axon tracing study (Wiencken-Barger et al. 2004) that differed in using fixed brains of $L1^{-/y}$ mice (n = 3) at an older age P14, which showed normal retrograde labeling of VB and dorsal LGN after injection of lipophilic dyes into S1 and V1, respectively. Thalamocortical axons in $CHL1^{-/-}$ mutants were retrogradely traced following dual injections of DiA into S1 and DiI into V1 (Fig. 2*C1*), as an example of our more extensive analysis (Wright et al. 2007). Results showed abnormal DiI labeling in VB thalamic nuclei, indicating caudally shifted projections from VB to V1. VB nuclei were colabeled with DiA, demonstrating the presence of normally projecting VB axons to S1. DiI labeling of the dorsal LGN indicated that LGN axons projected normally to V1 (Fig. 2*C1*). The projection of motor thalamic axons to M1 was unaffected by loss of CHL1 (Wright et al. 2007). This illustrates that loss of CHL1 causes caudal misprojection of contingents of VB axons to V1.

In $CHL1^{-/-}/L1^{-/y}$ mice injections (n = 4) of DiA into M1 (Fig. 2*D1*) resulted in normal labeling of thalamic motor nuclei (VA/VL) and not VB (VPM, VPL) or other nuclei in each case (Fig. 2*D2*). Injections of double mutants with DiI (n = 5) into S1 (Fig. 2*D3* and Supplementary Fig. 1) resulted in normal labeling of VB nuclei (VPM, VPL) and not dorsal LGN or other nuclei in each case (Fig. 2*D4*). Injections of DiI or DiA into V1 (n = 7) resulted in abnormal retrograde labeling of VB nuclei (VPM, VPL) (Fig. 2*D5*,*D7*) and motor nuclei (VA/VL) (Fig. 2*D6*,*D8*) in every case, in addition to normal labeling of the dorsal LGN (Fig. 2*D5*,*D7*). This suggested that the combined loss of CHL1 and L1 caused caudal misprojection of contingents of both motor and somatosensory thalamic axons to V1. Since the dorsal LGN is laterally positioned in the DT, the misprojection of VA axons, in particular, would also be shifted laterally to some extent.

Mistargeting of motor and somatosensory thalamic axons from VA/VL and VPM/VPL nuclei to V1 in the double mutants was fully penetrant (7 of 7 injections) and was not observed in single mutants (13/13 and in [Wright et al. 2007]). Caudal misprojections of motor thalamic axons were never seen in $CHL1^{-/-}$ single mutants (Wright et al. 2007). No rostrally directed misprojections were observed for any mutant. The location along both rostrocaudal and mediolateral DT axes of labeled nuclei in mutants appeared to correspond in general to the location of WT nuclei, despite the presence of misprojecting axons, although the spread of dye labeling in DT nuclei varied depending on the size of DiI/DiA injections. Because of this variation, any alterations in mediolateral axon projections, which are another important aspect of topography (Price et al. 2006; Bonnin et al. 2007; Powell et al. 2008), could not be accurately assessed. Serial coronal sections through the DT or cortex were examined in each case to assess the DiI/DiA injection sites and location of retrograde label throughout the DT, as shown for DiI injection into S1 of double mutants (Supplementary Fig. 1).

Chi-square analysis indicated that aberrant mapping of motor thalamic axons in $CHL1^{-/-}/L1^{-/y}$ double mutants to V1 and of somatosensory axons to V1 was significantly different from WT ($\chi^2 = 8.78$; $0.01 < P < 0.001$). Normal positioning of the V1/V2 boundary (Fig. 1*E–G*) in double mutants suggested that the posterior shift of VB axons to the visual cortex in double mutants was not likely to be due to altered cortical arealization in this region. Chi-square analysis further indicated that mistargeting of somatosensory thalamic axon contingents to V1 in $CHL1^{-/-}/L1^{-/y}$ double mutants was not significantly different from that in $CHL1^{-/-}$ mice (Wright et al. 2007) ($\chi^2 = 0.034$; $P > 0.5$), and thus is probably due to loss of CHL1 alone. In summary, these results showed that combined loss of L1 and CHL1 causes mistargeting specifically of motor thalamic axons from VA/VL to V1, whereas loss of either L1 or CHL1 alone has no effect on this projection.

L1 and CHL1 Mediate EphrinA5-Induced Growth Cone Collapse

The striking posterior shift of motor thalamic axons to the visual cortex in CHL1/L1 double mutants may be due to defective repellent thalamic axon guidance at the intermediate target, the VTe, where axons are initially sorted to areas of the cortex along the rostrocaudal axis (Dufour et al. 2003). A high caudal to low-rostral gradient of EphrinA5 in the VTe repels subpopulations of rostral thalamic axons, which express EphA receptors in a high-rostral countergradient, so that axons are guided to the motor cortex (Dufour et al. 2003). EphrinA5 in the VTe is a ligand for EphA3, EphA4, and EphA7, which are among the principal EphAs in the embryonic DT (Mackarehtschian et al. 1999; Dufour et al. 2003; Yun et al. 2003; Torii and Levitt 2005; Miller et al. 2006). To address whether CHL1 and/or L1 were capable of mediating the EphrinA5 repellent axon response, growth cone collapse assays were performed using dissociated cortical neurons from WT, $CHL1^{-/-}$ or $L1^{-/y}$ mutant embryos (E14.5). Primary cultures of cortical neurons from WT, $CHL1^{-/-}$, or $L1^{-/y}$ embryos were grown for 3 days followed by treatment for 30 min with 30 nM EphrinA5-Fc or nonimmune IgG as control. F-actin was labeled using rhodamine-labeled phalloidin, and axons were scored for growth cone collapse. Collapsed growth cones had a bullet-shaped morphology in contrast to uncollapsed growth cones, which were well spread and displayed numerous filopodia and lamellipodia.

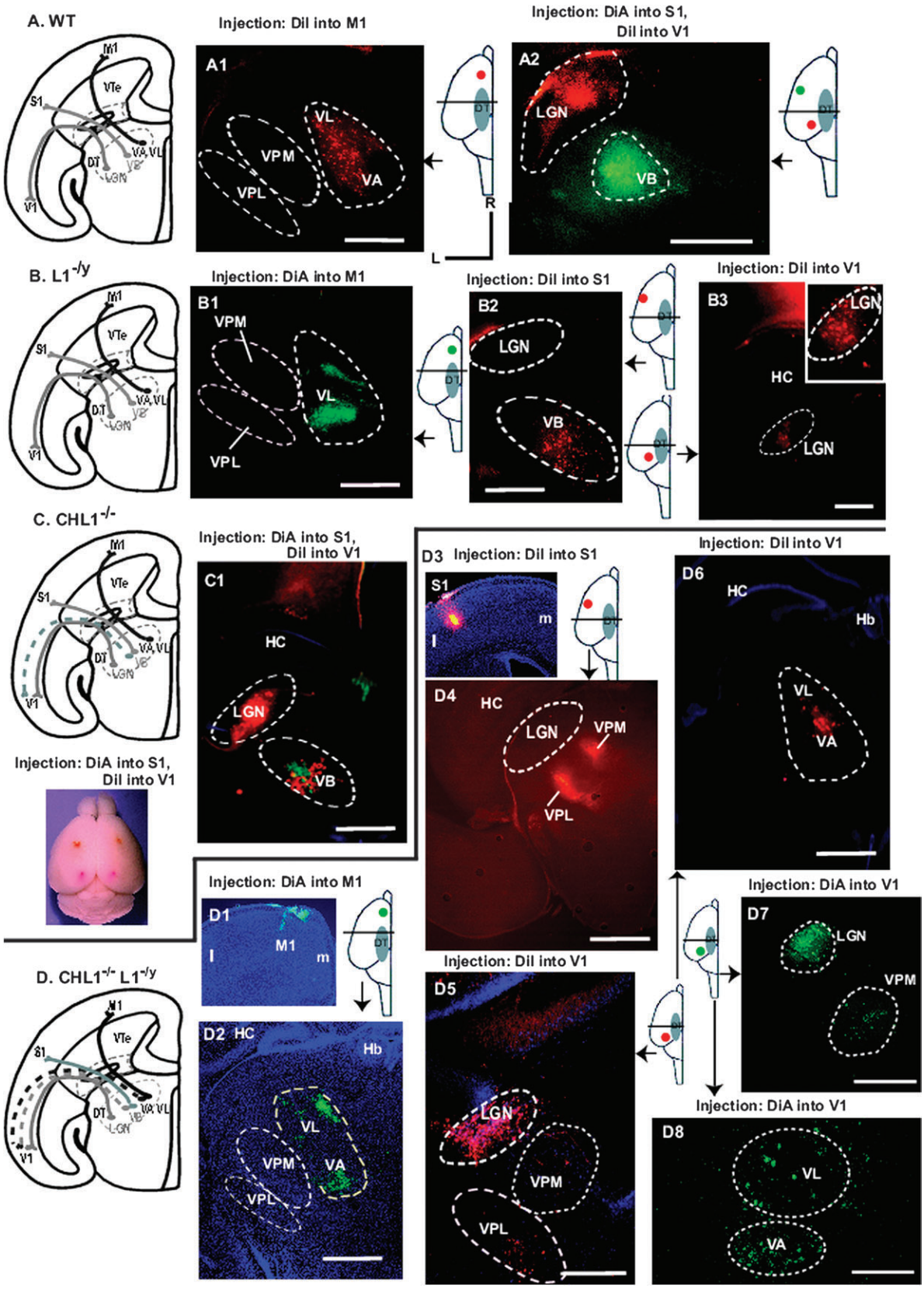

Figure 2. Retrograde tracing of thalamic axons from distinct cortical areas in WT, CHL1$^{-/-}$, L1$^{-/y}$, and CHL1$^{-/-}$/L1$^{-/y}$ double mutant mice (P7). (*A*) Scheme showing results of retrograde tracing of thalamocortical axons with DiI or DiA from different neocortical areas to distinct DT nuclei in WT mice. (*A1*) Retrograde labeling of WT motor thalamic nuclei (VA/VL) but not VB nuclei (VPM, VPL) is shown following injection of DiI into M1. (*A2*) Retrograde labeling of WT dorsal LGN and VB is shown following dual injection of DiI into V1 and DiA into S1. Orientation of all sections in Figure 2 are indicated (R, rostral; L, lateral). Injection sites and position of the sections are diagrammatically illustrated in each panel. (*B*) Scheme showing results of retrograde tracing of thalamocortical axons with DiI or DiA from different neocortical areas to distinct DT nuclei in L1$^{-/y}$ mice. (*B1*) Retrograde

EphrinA5-Fc induced robust growth cone collapse in WT cortical neurons, increasing the percent of collapsed growth cones by 50% over that of control neurons treated with nonimmune IgG (Fig. 3*A*,*B*). EphrinA5-Fc treatment of $L1^{-/y}$ cortical neurons resulted in a growth cone collapse response that was 18% lower than in WT neurons, while EphrinA5-Fc treatment of $CHL1^{-/-}$ cortical neurons resulted in a collapse response that was 31% lower than in WT neurons. Basal growth cone collapse in the presence of nonimmune IgG was equivalent for WT, $L1^{-/y}$, and $CHL1^{-/-}$ cortical neurons and was not different from the corresponding untreated cultures (not shown). In thalamic explants from WT E14.5 embryos, EphrinA5 tagged with AP (EphrinA5-AP) induced a pronounced growth cone collapse response relative to the Fc-AP–treated control (Fig. 3*C*,*D*). The collapse response was nearly equivalent for WT cortical and thalamic neurons. EphrinA5-AP–induced growth cone collapse in $CHL1^{-/-}$ thalamic explants was strongly abrogated compared with EphrinA5-AP–treated WT explants (Fig. 3*C*,*D*). Due to limitations in breeding L1 single and double mutants, it was not practical to assay the collapse response in thalamic explants for these mutant lines. In dissociated cultures of embryonic mouse cortical neurons, L1 and CHL1 were coexpressed in most of the cells (L1, 55/58 cells; CHL1, 56/58 cells) and were colocalized along neurites and growth cones (Fig. 3*E*). However, the intensity of immunofluorescence staining of each protein varied, and some neurites exhibit stronger staining for either L1 or CHL1 (Fig. 3*E*). Similarly, L1 and CHL1 were expressed and colocalized in neurites and growth cones in the vast majority of embryonic thalamic neurons in dissociated cultures (Fig. 3*E*).

In summary, CHL1 and L1 colocalized in growth cones of cortical and thalamic neurons and mediated EphrinA5-induced growth cone collapse in vitro. As CHL1, L1, and EphrinA5 (Henkemeyer et al. 1996) are expressed along the thalamocortical pathway at E14.5, they may regulate repellent guidance of thalamic axons to EphrinA5 in vivo.

L1 and CHL1 Selectively Associate with EphA Receptors

The findings that motor thalamic axons are shifted to the visual cortex in CHL1/L1 double mutants and that the EphrinA5 repellent response is impaired in cultured neurons lacking either L1 or CHL1 raises the hypothesis that L1-CAMs might interact with Eph receptors to mediate axon guidance of DT axons at the VTe. To test this hypothesis, potential interactions of CHL1 and L1 with EphA3, EphA4, EphA7, as well as EphB2, an EphrinA5 receptor expressed in E14.5 DT (Henkemeyer et al. 1996) were examined by coimmunoprecipitation. cDNA3 plasmids encoding CHL1 or L1 were cotransfected with EphA3, EphA4, EphA7, or EphB2 for transient expression in HEK293T cells. After 2 days, cell lysates were subjected to immunoprecipitation and immunoblotting. Each molecule was effectively expressed in the cells, as shown by immunoblotting of cell lysates (Fig. 4). L1 (~220 kDa doublet) coimmunoprecipitated with EphA3, EphA4, and EphA7 (Fig. 4*A*,*C*) but not with EphB2 (Fig. 4*D*), demonstrating an interaction of L1 with each of the principal EphrinA5 receptors expressed in the embryonic DT during thalamocortical axon pathfinding. Conversely, CHL1 coimmunoprecipitated with EphA7 (Fig. 4*C*) but not with EphA3, EphA4, or EphB2 (Fig. 4*A*,*B*, and *D*), thus demonstrating selectivity in the interaction of L1-CAMs with Eph receptors. EphA kinase activation may be required for recruitment of L1-CAMs, as EphA receptors are autoactivated when overexpressed (Pasquale 2005). L1 and CHL1 antibodies did not cross-react with EphA3, EphA4, or EphA7, as shown by immunoblotting of lysates from HEK293 cells transfected with each receptor or L1-CAM (Fig. 4*E*). These results demonstrate a specific interaction of L1 and CHL1 with individual EphA receptors. Such interactions were not observed by coimmunoprecipitation from embryonic DT lysates or whole brain, possibly due to a transient interaction or a requirement for ephrinA-induced activation of EphA signaling, as overexpression of EphAs in HEK293T cells routinely leads to ligand-independent autoactivation of EphA tyrosine kinase. Also the association may occur primarily in growth cones traversing the VTe, which constitute a very small amount of protein from embryonic brain or DT. The small size of the DT and VTe limit biochemical confirmation of the associations demonstrated in transfected HEK293 cells. It should be noted that L1 was shown to be recruited to EphA4 in platelet preparations, and this depended on activation of the kinase (Prevost et al. 2002).

Discussion

Here, we report a novel cooperative function for the L1-CAM family members CHL1 and L1 as mediators of topographic mapping of thalamic axons to the neocortex. Deletion of both CHL1 and L1 in a newly generated $CHL1^{-/-}/L1^{-/y}$ double mutant mouse disrupted area-specific targeting of thalamocortical axons in a manner distinct from that in either of the single mutants. Combined deletion of CHL1 and L1 caused contingents of axons from motor (VA/VL) and somatosensory (VB) thalamic nuclei to incorrectly target V1. L1 and CHL1 were coexpressed in the embryonic DT (E14.5) and colocalized on many axons within the thalamocortical projection as well as in neuronal cultures. A novel function for L1 and CHL1 was identified in mediating growth cone collapse to EphrinA5, a repellent cue important in thalamocortical axon guidance (Dufour et al. 2003; Cang et al. 2005), and each L1-CAM was found to associate with distinct but overlapping EphA receptor subclasses. These results suggest that functional complexes of L1-CAMs with EphAs and other repellent guidance receptors guide subpopulations of thalamic axons to distinct neocortical areas essential for thalamocortical connectivity.

labeling of VL but not VB nuclei (VPM, VPL) following injection of DiA into M1. (*B2*) Labeling of VB but not dorsal LGN following injection of DiI into S1. (*B3*) Retrograde labeling of dorsal LGN following injection of DiI into V1. (*C*) Scheme showing results of retrograde tracing of thalamocortical axons from different neocortical areas to distinct DT nuclei of $CHL1^{-/-}$ mice, in which axon contingents from the VB nucleus misproject caudally to V1. (*C1*) Retrograde labeling of VB and dorsal LGN following dual injections of DiA into S1 and DiI into V1. Neuronal soma in VB nuclei are inappropriately labeled with DiI. Injection sites are shown below the scheme. (*D*) Scheme showing results of retrograde tracing of thalamocortical axons from different neocortical areas to distinct DT nuclei of $CHL1^{-/-}/L1^{-/y}$ mice, in which axon contingents from VA/VL and VB nuclei misprojected caudally to V1. (*D1*) Injection site of DiA into M1 of the neocortex (m, medial; l, lateral). (*D2*) Retrograde labeling of VA and VL but not VB nuclei (VPM, VPL) following DiA injection into M1. 4′,6-diamidino-2-phenylindole staining shows hippocampus (HC) and habenula (Hb). (*D3*) Injection site of DiI into S1 (m, medial; l, lateral). (*D4*) Labeling of VPM and VPL nuclei following DiI injection into S1. (*D5*) Labeling of dorsal LGN, VPM, and VPL nuclei following DiI injection into V1. (*D6*) Labeling of VA and VL nuclei following DiI injection into V1. (*D7*) Labeling of VPM and dorsal LGN following DiA injection into V1. (*D8*) Labeling of VA and VL nuclei following DiA injection into V1. M1, primary motor cortex; S1, primary somatosensory cortex; V1, primary visual cortex. Magnification bars equal 500 μm in all panels except *D8* (300 μm).

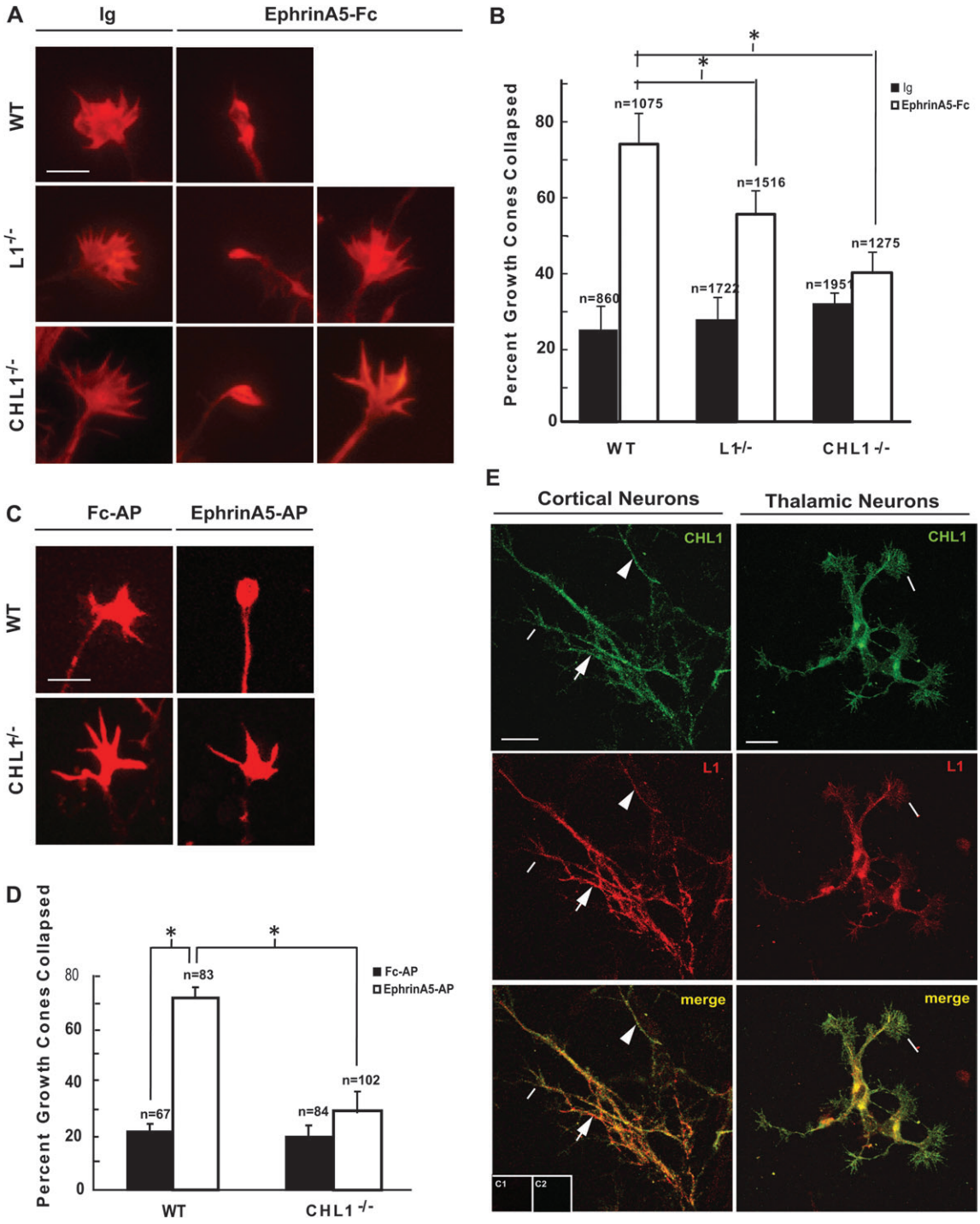

Figure 3. L1 and CHL1 mediate EphrinA5-induced growth cone collapse. (*A*) Dissociated cortical neurons from WT, $L1^{-/y}$, and $CHL1^{-/-}$ embryos (E14.5) were cultured for 3 days, treated with 30 nM EphrinA5 or 30 nM IgG for 30 min, fixed, and stained with phalloidin for visualizing F-actin. Images are representative examples of noncollapsed and collapsed growth cones scored following IgG or EphrinA5-Fc treatment. Magnification bar = 5 μm. (*B*) Quantification of growth cone collapse in dissociated cortical neuron cultures shown in *A*, in response to control IgG or EphrinA5-Fc. Percent growth cone collapse is expressed as the mean ± standard error of the mean (SEM) (n = number of growth cones scored). Asterisk indicates significant differences ($P < 0.05$; 2-tailed t-test). (*C*) WT and $CHL1^{-/-}$ thalamic explants (E14.5) were cultured for 3 days, treated with 30 nM EphrinA5-AP or 30 nM Fc-AP, fixed, and stained with phalloidin. Representative examples of noncollapsed and collapsed growth cones following control Fc-AP or EphrinA5-AP treatment. Magnification bar in *A* = 5 μm. (*D*) Quantification of growth cone collapse from thalamic explants in *C*, in response to EphrinA5-AP. Percent growth cone collapse is mean ± SEM. n = number of growth cones scored. Asterisk indicates significant differences in means ($P < 0.05$; 2-tailed t-test). (*E*) Immunofluorescence staining showing colocalization of L1 and CHL1 in embryonic mouse cortical and thalamic neurons in dissociated cultures. Colocalization was evident in growth cones of cortical and thalamic neurons (lines). Some neurites of cortical neurons appeared enriched for L1 (arrows) and others for CHL1 (arrowheads). Control staining without primary antibodies is shown for cortical neurons (C1) and thalamic neurons (C2). Magnification bars = 20 μm.

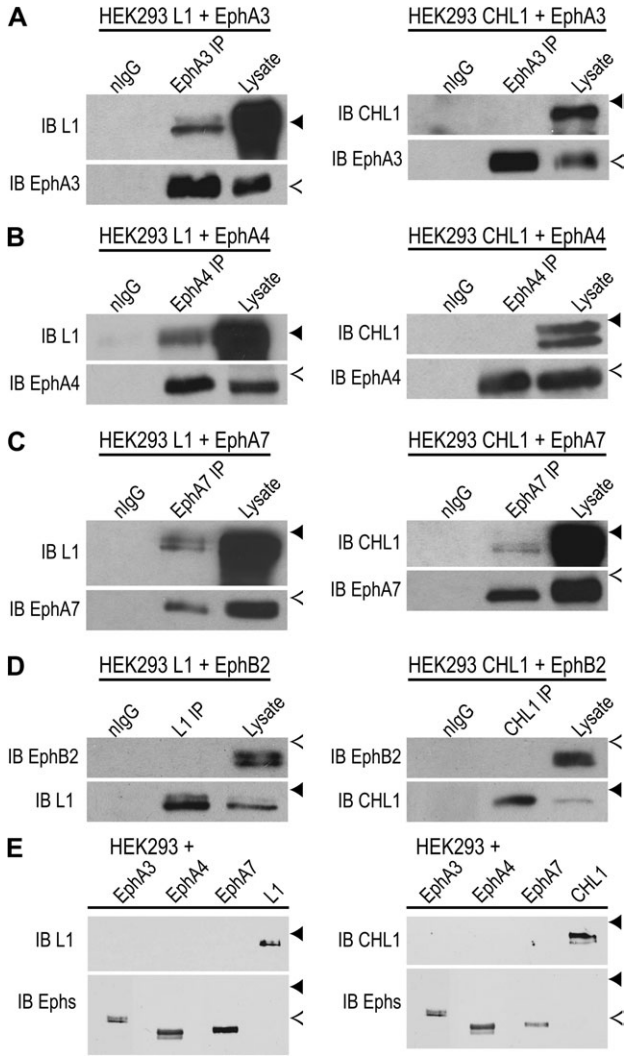

Figure 4. L1 and CHL1 associate with EphA receptors. (*A–D*) CHL1 or L1 were coexpressed with EphA3, EphA4, EphA7, or EphB2 from pcDNA3 plasmids after transient transfection of HEK293T cells. Lysates (500-μg protein) were immunoprecipitated (IP) using antibodies against EphA3, EphA4, EphA7, L1, CHL1, or normal IgG and immunoblotted (IB) for the indicated protein. Blots were reprobed with antibodies used for IP. IB of cell lysates (25 μg) confirmed expression of each protein in transfected cells. Position of molecular weight markers are indicated by solid arrowheads (250 kDa) and open arrowheads (130 kDa). L1 protein was detected in (*A*) EphA3, (*B*) EphA4, and (*C*) EphA7 immunoprecipitates. CHL1 was not detected in the immunoprecipitates of (*A*) EphA3 or (*B*) EphA4 but was detected in (*C*) EphA7 immunoprecipitates. EphB2 was not detected in either (*D*) L1 or CHL1 immunoprecipitates. (*E*) EphA3, EphA4, EphA7, L1, or CHL1 were expressed alone from pcDNA3 plasmids by transient transfection of HEK293T cells. Lysates (25-μg protein) were immunoblotted with antibodies L1 or CHL1 to demonstrate their specificity and showed no cross-reactivity with EphA receptors (upper panels). In lower panels, blots were stripped and reprobed with EphA-specific antibodies to confirm expression of each protein in transfected cells.

Axon tracing with DiI/DiA revealed a cooperative role for L1 and CHL1 in topographic mapping of contingents of thalamic axons from motor thalamic nuclei to the neocortex. CHL1$^{-/-}$/L1$^{-/y}$ double mutants exhibited a caudal shift of axons from VA/VL motor thalamic nuclei to V1, which was not observed in L1$^{-/y}$ or CHL1$^{-/-}$ single mutants (the present study and [Wright et al. 2007]). CHL1$^{-/-}$/L1$^{-/y}$ double mutants additionally showed a caudal shift of axon contingents from the VB complex to V1, but this was probably due to loss of CHL1, which resulted in the same misprojection as a consequence of impaired axon

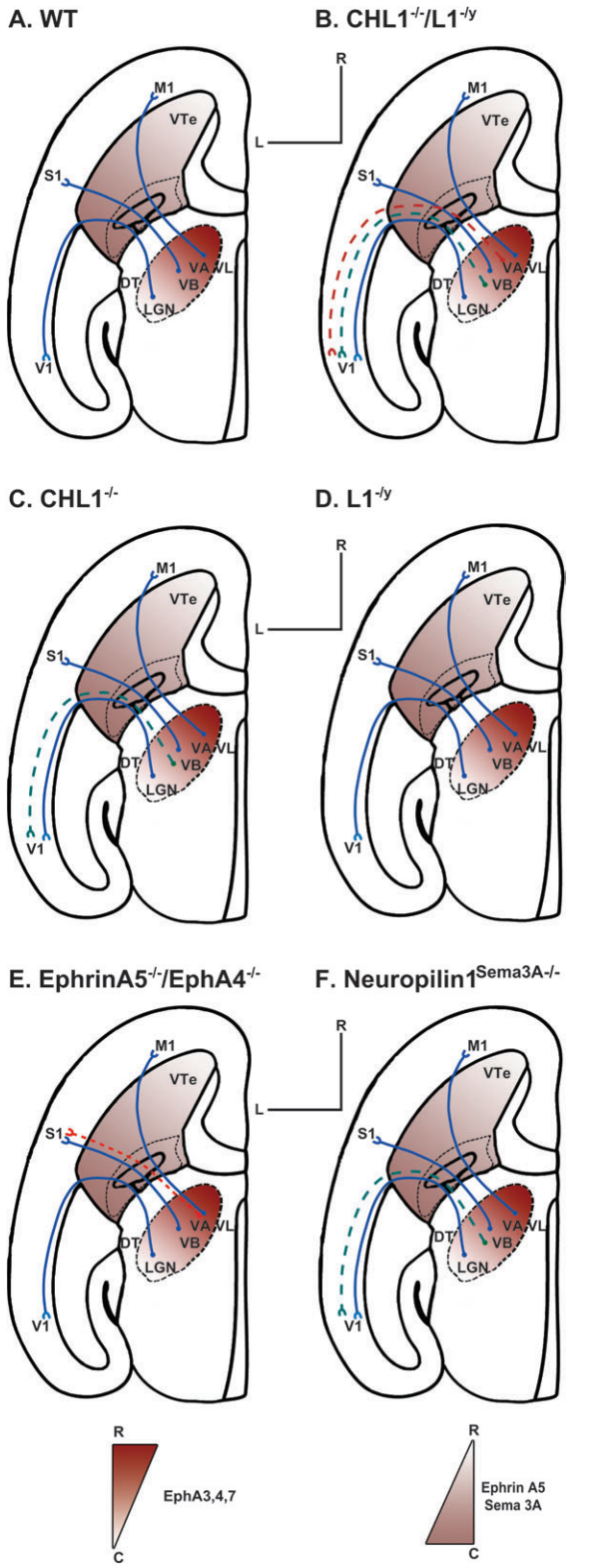

Figure 5. Schematic diagrams of thalamocortical trajectories based on axon tracing experiments in different mouse genotypes: (*A*) WT, (*B*) CHL1$^{-/-}$, (*C*) CHL1$^{-/-}$ L1$^{-/y}$, (*D*) L1$^{-/y}$, (*E*) EphrinA5$^{-/-}$/EphA4$^{-/-}$, and (*F*) Neuropilin-1 mutant defective in Sema3A binding. Normal projections are depicted as solid lines and misprojections as dashed lines. In CHL1$^{-/-}$/L1$^{-/y}$ and EphrinA5$^{-/-}$/EphA4$^{-/-}$ mutants, VA or VL axon contingents caudally misproject to V1 and VB, respectively. Note similar misprojection of VB axon contingents to V1 in CHL1$^{-/-}$ and Neuropilin1$^{Sema3A-/-}$ mutants. L1$^{-/y}$ mutants show normal projections. The location of rostrocaudal gradients of ephrinA5, Sema3A, and EphA3, 4, 7 are indicated by shading.

repulsion from the high-caudal Sema3A gradient in the VTe (Wright et al. 2007). Retrograde thalamocortical axon tracing in $L1^{-/y}$ mice at P5 showed that loss of L1 alone had no significant impact on thalamocortical mapping to these neocortical areas, in accord with axon tracing by other methods at P14 (Wiencken-Barger et al. 2004).

The finding that motor thalamic axons from VA/VL were caudally shifted in $CHL1^{-/-}/L1^{-/y}$ double mutant mice, suggests that these L1-CAMs may interact with the EphrinA/EphA system for repellent axon guidance of motor thalamic axons at the VTe. Such a role is in accord with colocalization of CHL1 and L1 on many thalamic axons within the VTe during thalamocortical axon sorting, their association with EphA receptors, and their requirement for EphrinA5-induced growth cone collapse. A high caudal to low-rostral gradient of EphrinA5 in the VTe directs rostral thalamic axons toward the rostral neocortex, through interactions with countergradients of EphA3, EphA4, and EphA7 on thalamocortical axons (Mackarehtschian et al. 1999; Dufour et al. 2003). As shown schematically (Fig. 5), $CHL1^{-/-}/L1^{-/y}$ double mutants exhibited a more severe caudal mistargeting phenotype in which contingents of VA/VL axons caudally misprojected to V1, compared with mutants lacking both EphrinA5 and EphA4 (or mutants lacking EphA7) (Dufour et al. 2003), in which motor thalamic axons are caudally shifted only to S1 (Dufour et al. 2003). Cooperative signaling involving both CHL1/EphA7 and L1/EphA3,-A4,-A7 acting as coreceptors for EphrinA5 would be expected to exert a stronger effect than single coreceptors in repelling motor thalamic axons from the posterior high EphrinA5 gradient in the VTe. Retrograde tracing did not allow us to assess subtle mediolateral shifts of mutant DT axons, which could also be affected by ephrinA/EphA signaling or to determine where in the thalamocortical trajectory misguidance occurred.

Our results do not implicate a cooperative role for L1 and CHL1 in transducing signals for Sema3A-induced axon repulsion, although L1, like CHL1, binds Neuropilin-1 and serves as a coreceptor for Sema3A in growth cone collapse (Bechara et al. 2008). Sema3A acts as a caudal repellent for VB axons in the VTe mediated by CHL1 interaction with Neuropilin-1 (Wright et al. 2007). Like CHL1 null mutants, mice expressing Neuropilin-1 mutated in the Sema3A binding site (Wright et al. 2007) show caudal shifts of VB axon contingents to V1 (Fig. 5). Loss of CHL1 alone (Wright et al. 2007) but not L1 alone (shown here and [Wiencken-Barger et al. 2004]) caused VB axons to caudally misproject to V1; thus, the caudal mistargeting of VB axons to V1 observed in the double mutant is likely due to loss of CHL1 alone.

L1 and CHL1 may also contribute to EphrinA/EphA-mediated inter-areal and intra-areal targeting of thalamocortical axons in the neocortex as well as the corticothalamic projection. EphrinA5 gradients are expressed in complex patterns in the developing neocortex (Mackarehtschian et al. 1999; Yun et al. 2003), where they may act as cortical cues for guidance of thalamic axons to correct cortical areas. EphrinAs have also been shown to regulate intra-areal thalamocortical axon targeting within V1 (Cang et al. 2005; Pfeiffenberger et al. 2005). Furthermore, EphA7 is required for reciprocal corticothalamic axon targeting within thalamic nuclei (Torii and Levitt 2005). CHL1 and L1 might contribute to the corticothalamic projection, as CHL1 binds EphA7, and loss of L1 causes hyperfasciculation and reduced numbers of corticothalamic axons, with fewer axons reaching the DT (Ohyama et al. 2004). If corticothalamic axons reciprocally influence thalamocortical targeting, as postulated in the "handshake" hypothesis (Molnar et al. 1998), reduced numbers of corticothalamic axons reaching the DT in L1-CAM mutant mice, might cause DT axon subpopulations to misproject. Due to limited availability and inefficient breeding of $CHL1^{-/-}/L1^{-/y}$ double mutant mice, it was not feasible to analyze thalamic axon guidance at embryonic stages to assess their function either at the VTe or dorsal telencephalon. Furthermore, we do not know if the observed mapping phenotype of double mutants at P7 is stable or transient, as these mice are difficult to maintain at older ages.

Both L1 and CHL1 mediated growth cone collapse to EphrinA5 in cortical and thalamic neurons, however, they displayed specificity in their interactions with EphA subclasses. L1 associated with EphA3, -A4, and -A7, whereas CHL1 preferentially associated with EphA7. L1-CAMs do not seem to control repellent responses to all cue, as L1 mediates growth cone collapse to Sema3A but not Sema3B or Sema3E (Castellani et al. 2000). In the mouse thalamocortical pathway, distinctive patterns of expression have been demonstrated for EphrinAs (EphrinA3, -A4, and -A5 [Mackarehtschian et al. 1999]) and EphA receptors (EphA3, -A4, and -A7 [Mackarehtschian et al. 1999; Torii and Levitt 2005; Uziel et al. 2006]). Interestingly, EphA4 and EphA7 have been shown to selectively bind different EphrinAs (Janis et al. 1999). Since L1-CAMs mediate EphrinA-induced growth cone collapse, the interaction of L1 and CHL1 with distinct EphA receptor classes might confer differential responsiveness of growth cones within neuronal subpopulations to different EphrinA gradients in the developing brain, enabling more precise thalamocortical axon targeting.

Funding

National Institutes of Health (NS049109 and MH064056 to P.F.M.); Deutsche Forschungsgemeinschaft (BA 1674/2-2 to U.B.); New Jersey Commission for Scientific Research (M.S.).

Supplementary Material

Supplementary material can be found at: http://www.cercor.oxfordjournals.org/

Notes

Conflict of Interest: None declared.

References

Agmon A, Yang LT, Jones EG, O'Dowd DK. 1995. Topological precision in the thalamic projection to neonatal mouse barrel cortex. J Neurosci. 15:549–561.

Bartsch U, Faissner A, Trotter J, Dorries U, Bartsch S, Mohajeri H, Schachner M. 1994. Tenascin demarcates the boundary between the myelinated and nonmyelinated part of retinal ganglion cell axons in the developing and adult mouse. J Neurosci. 14:4756–4768.

Bechara A, Nawabi H, Moret F, Yaron A, Weaver E, Bozon M, Abouzid K, Guan JL, Tessier-Lavigne M, Lemmon V, et al. 2008. FAK-MAPK-dependent adhesion disassembly downstream of L1 contributes to semaphorin3A-induced collapse. EMBO J. 27: 1549–1562.

Bonnin A, Torii M, Wang L, Rakic P, Levitt P. 2007. Serotonin modulates the response of embryonic thalamocortical axons to netrin-1. Nat Neurosci. 10:588–597.
Buhusi M, Schlatter MC, Demyanenko GP, Thresher R, Maness PF. 2008. L1 interaction with ankyrin regulates mediolateral topography in the retinocollicular projection. J Neurosci. 28:177–188.
Cang J, Kaneko M, Yamada J, Woods G, Stryker MP, Feldheim DA. 2005. Ephrin-as guide the formation of functional maps in the visual cortex. Neuron. 48:577–589.
Castellani V, Chedotal A, Schachner M, Faivre-Sarrailh C, Rougon G. 2000. Analysis of the L1-deficient mouse phenotype reveals cross-talk between Sema3A and L1 signaling pathways in axonal guidance. Neuron. 27:237–249.
Cohen NR, Taylor JSH, Scott LB, Guillery RW, Soriano P, Furley AJW. 1998. Errors in corticospinal axon guidance in mice lacking the neural cell adhesion molecule L1. Curr Biol. 8: 26–33.
Dahme M, Bartsch U, Martini R, Anliker B, Schachner M, Mantei N. 1997. Disruption of the mouse L1 gene leads to malformations of the nervous system. Nat Genet. 17:346–349.
Demyanenko G, Tsai A, Maness PF. 1999. Abnormalities in neuronal process extension, hippocampal development, and the ventricular system of L1 knockout mice. J Neurosci. 19:4907–4920.
Demyanenko GP, Maness PF. 2003. The L1 cell adhesion molecule is essential for topographic mapping of retinal axons. J Neurosci. 23:530–538.
Demyanenko GP, Schachner M, Anton E, Schmid R, Feng G, Sanes J, Maness PF. 2004. Close homolog of L1 modulates area-specific neuronal positioning and dendrite orientation in the cerebral cortex. Neuron. 44:423–437.
Dufour A, Seibt J, Passante L, Depaepe V, Ciossek T, Frisen J, Kullander K, Flanagan JG, Polleux F, Vanderhaeghen P. 2003. Area specificity and topography of thalamocortical projections are controlled by ephrin/Eph genes. Neuron. 39:453–465.
Feng G, Mellor RH, Bernstein M, Keller-Peck C, Nguyen QT, Wallace M, Nerbonne JM, Lichtman JW, Sanes JR. 2000. Imaging neuronal subsets in transgenic mice expressing multiple spectral variants of GFP. Neuron. 28:41–51.
Flanagan JG, Cheng HJ. 2000. Alkaline phosphatase fusion proteins for molecular characterization and cloning of receptors and their ligands. Methods Enzymol. 327:198–210.
Fransen E, D'Hooge R, Van Camp G, Verhoye M, Sijbers J, Reyniers E, Soriano P, Kamiguchi H, Willemsen R, Koekkoek SK, et al. 1998. L1 knockout mice show dilated ventricles, vermis hypoplasia and impaired exploration patterns. Hum Mol Genet. 7:999–1009.
Frints SGM, Marynen P, Hartmann D, Fryns JP, Steyaert J, Schachner M, Rolf B, Craessaerts K, Snellinx A, Hollanders K, et al. 2003. CALL interrupted in a patient with nonspecific mental retardation: gene dosage-dependent alteration of murine brain development and behavior. Hum Mol Genet. 12:1463–1474.
Fukuda T, Kawano H, Ohyama K, Li HP, Takeda Y, Oohira A, Kawamura K. 1997. Immunohistochemical localization of neurocan and L1 in the formation of thalamocortical pathway of developing rats. J Comp Neurol. 382:141–152.
Guseva D, Angelov DN, Irintchev A, Schachner M. 2009. Ablation of adhesion molecule L1 in mice favours Schwann cell proliferation and functional recovery after peripheral nerve injury. Brain. 132: 2180–2195.
Henkemeyer M, Orioli D, Henderson JT, Saxton TM, Roder J, Pawson T, Klein R. 1996. Nuk controls pathfinding of commissural axons in the mammalian central nervous system. Cell. 86:35–46.
Irintchev A, Koch M, Needham LK, Maness P, Schachner M. 2004. Impairment of sensorimotor gating in mice deficient in the cell adhesion molecule L1 or its close homologue, CHL1. Brain Res. 1029:131–134.
Janis LS, Cassidy RM, Kromer LF. 1999. Ephrin-A binding and EphA receptor expression delineate the matrix compartment of the striatum. J Neurosci. 19:4962–4971.
Kenwrick S, Watkins A, Angelis ED. 2000. Neural cell recognition molecule L1: relating biological complexity to human disease mutations. Hum Mol Genet. 9:879–886.
Kolata S, Wu J, Light K, Schachner M, Matzel LD. 2008. Impaired working memory duration but normal learning abilities found in mice that are conditionally deficient in the close homolog of L1. J Neurosci. 28:13505–13510.
Kudo C, Ajioka I, Hirata Y, Nakajima K. 2005. Expression profiles of EphA3 at both the RNA and protein level in the developing mammalian forebrain. J Comp Neurol. 487:255–269.
Mackarehtschian K, Lau CK, Caras I, McConnell SK. 1999. Regional differences in the developing cerebral cortex revealed by ephrin-A5 expression. Cereb Cortex. 9:601–610.
Maness PF, Schachner M. 2007. Neural recognition molecules of the immunoglobulin superfamily: signaling transducers of axon guidance and neuronal migration. Nat Neurosci. 10:19–26.
Miller CR, Dunham CP, Scheithauer BW, Perry A. 2006. Significance of necrosis in grading of oligodendroglial neoplasms: a clinicopathologic and genetic study of newly diagnosed high-grade gliomas. J Clin Oncol. 24:5419–5426.
Molnar Z, Adams R, Blakemore C. 1998. Mechanisms underlying the early establishment of thalamocortical connections in the rat. J Neurosci. 18:5723–5745.
Molnar Z, Higashi S, Lopez-Bendito G. 2003. Choreography of early thalamocortical development. Cereb Cortex. 13:661–669.
Montag-Sallaz M, Schachner M, Montag D. 2002. Misguided axonal projections, neural cell adhesion molecule 180 mRNA upregulation, and altered behavior in mice deficient for the close homolog of L1. Mol Cell Biol. 22:7967–7981.
Needham LK, Thelen K, Maness PF. 2001. Cytoplasmic domain mutations of the L1 cell adhesion molecule reduce L1-ankyrin interactions. J Neurosci. 21:1490–1500.
Nikonenko AG, Sun M, Lepsveridze E, Apostolova I, Petrova I, Irintchev A, Dityatev A, Schachner M. 2006. Enhanced perisomatic inhibition and impaired long-term potentiation in the CA1 region of juvenile CHL1-deficient mice. Eur J Neurosci. 23:1839–1852.
Ohyama K, Tan-Takeuchi K, Kutsche M, Schachner M, Uyemura K, Kawamura K. 2004. Neural cell adhesion molecule L1 is required for fasciculation and routing of thalamocortical fibres and corticothalamic fibres. Neurosci Res. 48:471–475.
Pasquale EB. 2005. Eph receptor signalling casts a wide net on cell behaviour. Nat Rev Mol Cell Biol. 6:462–475.
Paxinos G, Halliday G, Watson C, Koutcherov Y, Wang H. 2007. Atlas of the developing mouse brain. 1st ed. Amsterdam: Elsevier.
Pfeiffenberger C, Cutforth T, Woods G, Yamada J, Renteria RC, Copenhagen DR, Flanagan JG, Feldheim DA. 2005. Ephrin-As and neural activity are required for eye-specific patterning during retinogeniculate mapping. Nat Neurosci. 8:1022–1027.
Powell AW, Sassa T, Wu Y, Tessier-Lavigne M, Polleux F. 2008. Topography of thalamic projections requires attractive and repulsive functions of Netrin-1 in the ventral telencephalon. PLoS Biol. 6:e116.
Pratte M, Rougon G, Schachner M, Jamon M. 2003. Mice deficient for the close homologue of the neural adhesion cell L1 (CHL1) display alterations in emotional reactivity and motor coordination. Behav Brain Res. 147:31–39.
Prevost N, Woulfe D, Tanaka T, Brass LF. 2002. Interactions between Eph kinases and ephrins provide a mechanism to support platelet aggregation once cell-to-cell contact has occurred. Proc Natl Acad Sci U S A. 99:9219–9224.
Price DJ, Kennedy H, Dehay C, Zhou L, Mercier M, Jossin Y, Goffinet AM, Tissir F, Blakey D, Molnar Z. 2006. The development of cortical connections. Eur J Neurosci. 23:910–920.
Runker AE, Bartsch U, Nave KA, Schachner M. 2003. The C264Y missense mutation in the extracellular domain of L1 impairs protein trafficking in vitro and in vivo. J Neurosci. 23:277–286.
Suh LH, Oster SF, Soehrman SS, Grenningloh G, Sretavan DW. 2004. L1/Laminin modulation of growth cone response to EphB triggers growth pauses and regulates the microtubule destabilizing protein SCG10. J Neurosci. 24:1976–1986.
Torii M, Levitt P. 2005. Dissociation of corticothalamic and thalamocortical axon targeting by an EphA7-mediated mechanism. Neuron. 48:563–575.

Uziel D, Garcez P, Lent R, Peuckert C, Niehage R, Weth F, Bolz J. 2006. Connecting thalamus and cortex: the role of ephrins. Anat Rec Part A. 288A:135–142.

Vanderhaeghen P, Polleux F. 2004. Developmental mechanisms patterning thalamocortical projections: intrinsic, extrinsic and in between. Trends Neurosci. 27:384–391.

Wiencken-Barger AE, Mavity-Hudson J, Bartsch U, Schachner M, Casagrande VA. 2004. The role of L1 in axon pathfinding and fasciculation. Cereb Cortex. 14:121–131.

Wright AG, Demyanenko GP, Powell A, Schachner M, Enriquez-Barreto L, Tran TS, Polleux F, Maness PF. 2007. Close homolog of L1 and neuropilin 1 mediate guidance of thalamocortical axons at the ventral telencephalon. J Neurosci. 27: 13667–13679.

Yun ME, Johnson RR, Antic A, Donoghue MJ. 2003. EphA family gene expression in the developing mouse neocortex: regional patterns reveal intrinsic programs and extrinsic influence. J Comp Neurol. 456:203–216.